PAPER ID: 1019
DOI: 10.18462/iir.gl.2020.1019

Experimental evaluation of a water based high temperature heat pump with novel high pressure lift turbo compressors

Espen VERPE [(a)], Christian Schlemminger[(a)], Michael Bantle[(a)], Marcel Ahrens[(b)]

(a) SINTEF Energy Research, Trondheim, 7034, Norway, espen.h.verpe@sintef.no
(b) Norwegian University of Science and Technology Trondheim, 7034, Norway, marcel.u.ahrens@ntnu.no

ABSTRACT

This paper evaluates a water based (R718) high temperature heat pump with novel high-pressure lift turbo compressors. The first stage turbo compressor is designed for steam compression and the second stage is designed for air, both are based on economic standard components from the automotive industry. A 500 kW compressor test rig was built by SINTEF to test the 2-stage configuration in superheated steam conditions. Compressor efficiency and system COP was calculated based on measurements from the test rig. Also, compressor maps for the two compressors was created. For the 1st stage compressor, the maximum isentropic efficiency was 67% and maximum pressure ratio 2.4. The second stage yielded 77% and 2.0. The two-stage configuration was able to produce 4.23 bar steam, from atmospheric inlet conditions. The system COP corresponded to 4.5 and a Carnot efficiency of 49.5 %.

Keywords: Heat pumps, HTHP, Water R718, turbo compressor, energy efficiency, steam production

1. INTRODUCTION

Industrial heat pumps do not normally operate with a supply temperature above 100 °C. However, recent technology advancement in the field of high temperature heat pumps (HTHP) has increased the number of both market ready and demonstrated units. A paper from (Arpagaus, 2018) listed some of the market available HTHP delivering heat in the range of 110 °C to 165 °C. In addition to this, Olvondo Technology, EPCON Evaporation Technology offers HTHP in medium (700 kW) and large scale (several MW), respectively.

The choice of working fluids for a HTHP is limited. Water (R718) is one of the few alternatives that is not only thermodynamically effective but also environmental-friendly, non-flammable, non-toxic and cost-effective (Larminat et al., 2014). Since water vapor (steam) is used as energy source in numerous plants, its industrial acceptance is very high. Disadvantages include high specific volumes at temperatures generally available from a waste heat source (60 °C to 100 °C), as well as a large volume change and superheating during compression (Šarevski, 2017).

Numerous industrial processes exists with heat demands at temperatures above 100 °C, such as drying, evaporation, distillation, for which steam is used as a heat transport medium (Elmegaard et al., 2017). This enables the use of the technology called mechanical vapor recompression (MVR), which drastically reduces the energy consumption. In the case of drying, an energy reduction of 70 % to 80 % can be expected (Lopez, 2003) compared to hot air dyers.

Research projects are aiming for industrial demonstrators within HTHP, such as DryFiciency, PACO project and a demonstrator from shanghai university (Wu, 2018). Booth the PACO project and the heat pump developed in Shanghai uses steam as working fluid. DryFiciency is aiming for 3 demonstrators in which one of them is an open loop steam heat pump (MVR), which uses the technology described in this paper.

SINTEF has done previous research on developing and testing high speed steam turbo compressors, where results can be found in (Bantle, 2019). Other recent research on turbo compressors is done by (Madsboell, 2015) and (Weel, 2012). This paper stands out as the compressor described in this paper is specially designed to compress steam, whereas the others use compressor wheels originally designed for air compression.

http://dx.doi.org/10.18462/iir.gl.2020.1019

2. METHOD AND MATERIALS

2.1. Test rig setup

In Fig. 1 the essential components and measuring points of the test facility are presented. The two-stage turbo-compressor test rig is designed to simulate an industrial steam dryer, providing up to one ton of excess steam per hour at atmospheric pressure and 10 K to 20 K superheat. Drying conditions are simulated by means of a steam generator and steam cooler.

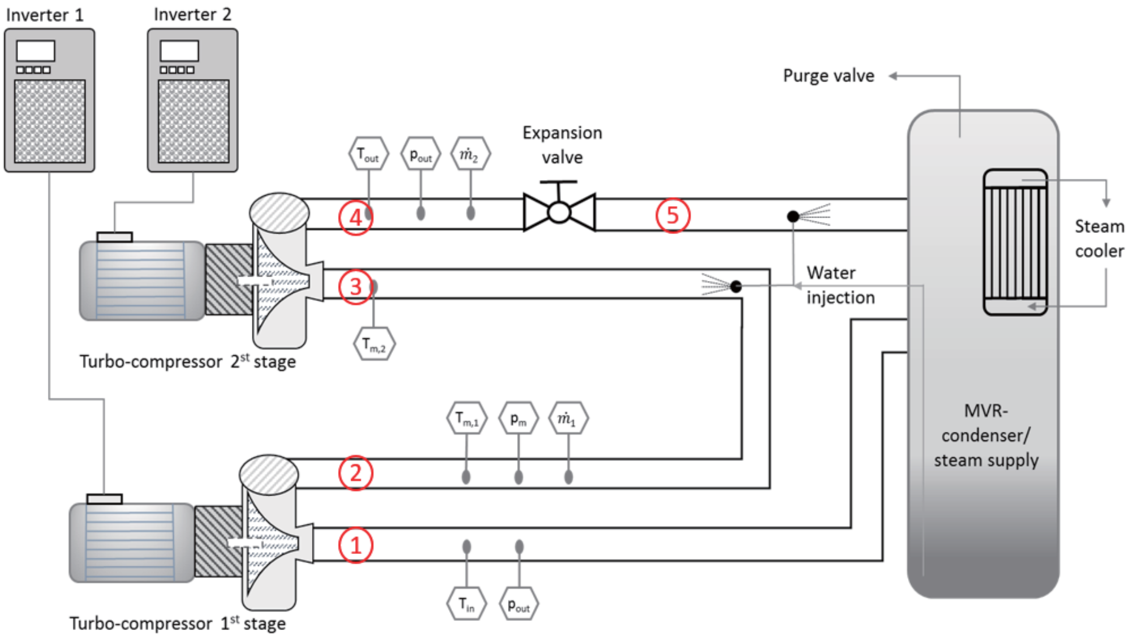

Figure 1: Simplified experimental setup with main components and measurement equipment

The test rig is operated in superheated steam condition, and only parts of the steam is condensed in order to maintain atmospheric pressure in the steam generator tank. This can be seen from the "triangle cycle" in Figure 2. The mass flow, and therefore the condensing pressure, is controlled by the expansion valve after the second compressor. Desuperheating is done by direct injection of water into the superheated steam, which results in long pipes to fully evaporate the injected water before the next compressor. A separator is installed between the first desuperheater and the second compressor to ensure no liquid droplets into the compressor.

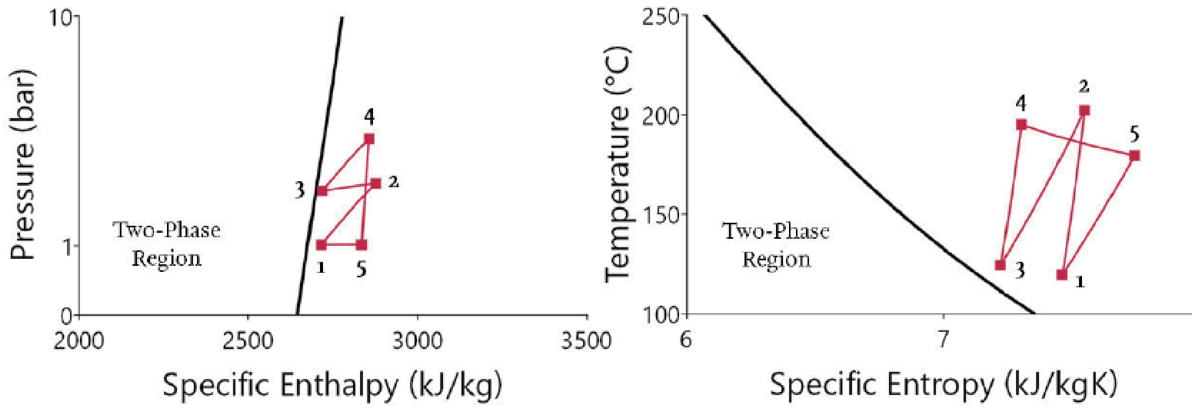

Figure 2: Illustration of the PH and TS diagram for the steam in the compressor test rig

2.2. Turbo compressors

The turbo compressor technology used in the experiments is based on mass produced turbochargers from the automotive industry, and prototypes have been developed by the Danish company ROTREX™. The compressor consists of mainly three parts, a 70 kW brushless DC engine, a traction drive gear box and an

http://dx.doi.org/10.18462/iir.gl.2020.1019

impeller. The impeller housing is mounted with an airgap to the gear box in order to reduce the amount of heat transfer from the compressed steam to the rest of the compressor.

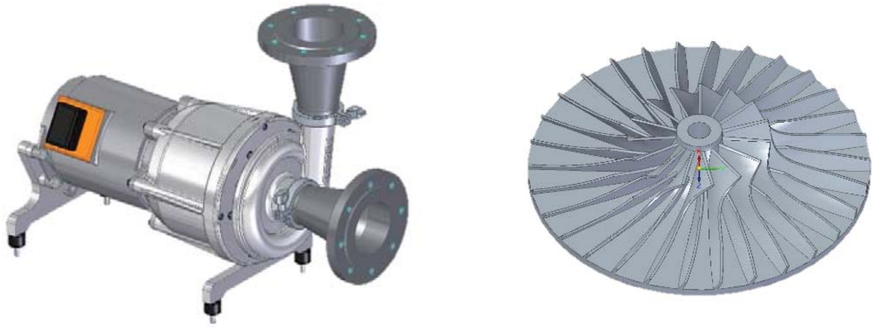

Figure 3: Design of a high speed turbo compressor prototype by Rotrex, along with the 14.6 cm impeller

Unlike the other high-speed steam turbo compressor tests previously done at SINTEF, the 1st stage impeller is designed for steam compression. Furthermore, improved oil cooling is done by an internal circulating oil pump, which is cooled in series with the electric motor with an external water loop.

Table 1: Design specifications of the two specially designed steam turbo compressors

Design specifications	Stage 1	Stage 2
Media	steam	air
Pressure ratio	3.2	2.0
Inlet volume flow	1230 m^3/h	470 m^3/h
Impeller speed	80 000 RPM	90 000 RPM
Gear ratio	6	7.5
Inducer diameter	61.3 mm	52.8 mm
Exducer diameter	145.9 mm	107.2 mm
Mach number	1.275	-

2.3. Experimental procedure

The measurement equipment showed in Table 2 was logged every 10 seconds during the experiments. Each operating point was stable for at least 10 minutes, in terms of mass flow (± 1 %), suction /discharge temperature (± 2 K) and suction/discharge pressure (± 0.02 bar). For a given compressor speed, the expansion valve was incrementally closed between each operating point, reducing the mass flow rate and increasing the pressure ratio. Doing so, the speed lines in the compressor maps, illustrated in Figure 4, are formed and the isentropic efficiency can be calculated using the experimental data.

Table 2: Measurement equipment and their accuracy in the test rig

Name	Accuracy	Range	Position
Temperature Transmitter (PT100)	±0.75°C	0 – 300 °C	Before and after each compressor (in pairs)
Pressure Transmitter 1st stage suction 1st stage discharge 2nd stage suction 2nd stage discharge	±0.75% of full scale	 0-1.6 bar 0-4.0 bar 0-4.0 bar 0-10.0 bar	Before and after each compressor
Differential pressure	±0.75% of full scale	0-2 bar	Around orifice plates
Orifice plate	±0.75%		After compressor 1 and 2
Power meters	±0.5%		On power supply before inverter

2.4. Compressor performance mapping

A compressor map is a commonly used graph to represent, compare and analyse the performance at various operating conditions. Figure 4 shows a typical performance map for turbo-compressors illustrating the relationship between mass/volume flow rate, pressure ratio, isentropic efficiency and impeller speed. Unstable operating areas are represented by the "surge line" and "choke line". Surge behaviour occurs when the fluid

http://dx.doi.org/10.18462/iir.gl.2020.1019

flows back from the high-pressure to the low-pressure side, while choke behaviour is characterised by a rapid drop in pressure ratio and efficiency.

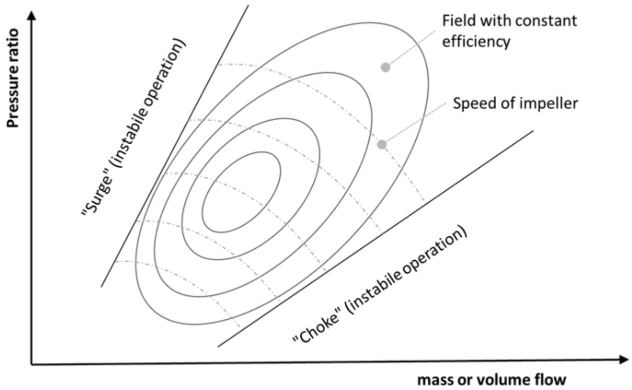

Figure 4: Schematic representation of a typical performance map for a turbo compressor

All measured operating points are calculated back to a standardised reference point (P_{ref}, T_{ref}). This is especially important for steam (R718) whose density is strongly reduced with reduced pressure. It is also recommended to adjust the impeller speed to correct for temperature influence (Hafaifa et al., 2014). These corrections enable a comparison of different operating points in the same performance map. The isentropic efficiency, η_{is}, is calculated from the ratio of enthalpy difference over the compressor for isentropic and real operating conditions (given from temperature and pressure measurement at inlet and outlet).

$$\eta_{is} = \frac{h_{out,is} - h_{in}}{h_{out} - h_{in}} \tag{1}$$

The pressure ratio, PR, is the ratio of discharge and suction pressure of each compressor

$$PR = \frac{p_{out}}{p_{in}} \tag{2}$$

The mass flow in the compressor, presented in the performance map, is calculated back to the suction side reference point, which was set to 1.013 bar and 120 °C (corresponds to dryer condition):

$$\dot{m}_{red} = \dot{m} \cdot \frac{\sqrt{(T_{in}/T_{ref})}}{(p_{in}/p_{ref})} \tag{3}$$

The corrected impeller speed, N, is given in Eq. 5, where N_{set} is the set speed at the inverter.

$$N_{red} = \frac{N_{set}}{\sqrt{(T_{in}/T_{ref})}} \tag{5}$$

The speed corrected pressure ratio and mass flow rate can be calculated as

$$PR_{rel} = PR \cdot \frac{N_{set}}{N_{red}} \quad and \quad \dot{m}_{rel} = \dot{m}_{red} \cdot \frac{N_{set}}{N_{red}}$$

To calculate the COP of the drying system, the enthalpy difference from the outlet of the 2nd compressor, $\mathrm{h}_{2,\mathrm{out}}$, and saturated liquid, $\mathrm{h}_{2,\mathrm{sat\,liq}}$ for the same pressure is assumed to equal the delivered heat.

$$\mathrm{COP}_{dryer} = \frac{\dot{Q}_c}{\mathrm{P}_{el}} = \frac{\dot{\mathrm{m}}_{steam} \cdot (\mathrm{h}_{2,\mathrm{out}} - \mathrm{h}_{2,\mathrm{sat\,liq}})}{\mathrm{P}_{el}}$$

3. RESULTS

3.1. Compressor maps

The most notable difference in the compressor maps, Figure 5, is the contrast in isentropic efficiency. The impeller specially designed for high pressure lifts in steam atmosphere has lower isentropic efficiency. The measurements reviled a slightly lower pressure ratio than designed. However, the pressure increase is approximately 0.4 bar higher than for the previously tested compressor in (Bantle, 2019). Isentropic efficiency

http://dx.doi.org/10.18462/iir.gl.2020.1019

varied between 57% and 65%, and a pressure ratio of 2.4 was reached at 90% speed. The surge line proved to be linear.

The isentropic efficiency of the second stage compressor, originally designed for air, has a higher isentropic efficiency, reaching 77% in the leftmost region. The maximum pressure ratio was 2.0, also at 90% speed. The maximum speed could not be reached due to high motor temperature in the first stage, and high oil temperature on the second stage. Choke conditions where reached without reducing the backpressure, as can be clearly seen on the drop in pressure ratio and isentropic efficiency.

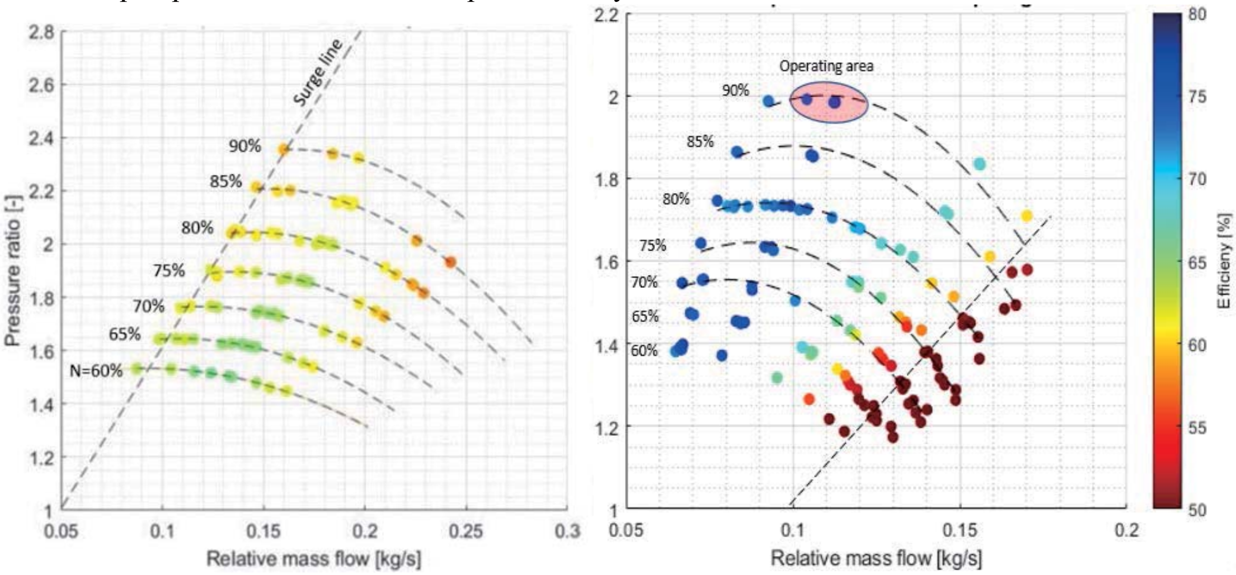

Figure 5: Compressor maps using equations 1-6 for the first (left) and second (right) stage compressor

3.2. System Efficiency

The two-stage turbo compressor setup is soon to be tested in an industrial superheated steam dryer, having a designed evaporative rate of around 800 kg/h, illustrated in Figure 6. The test setup reached a total pressure ratio of 4.23, including all pressure losses as seen in Table 3. The total COP of the system, including losses in pressure, heat, inverter and motor was calculated to be 4.54. Note that the tested system does not evaporate or condense the refrigerant (heat exchanger losses are not included).

Table 3: KPIs of the 2-stage turbo compressor heat pump at ideal drying condition

Speed	Speed	$\dot{m}$	PR	T_{sat}	T_{lift}	$\dot{Q}_c$	COP	COP_{Carnot}	η_{system}
RPM	%	kg/s	-	°C	K	kW	-	-	%
72000/81000	90/90	0.21	4.23	146	45.6	494	4.54	9.18	49.4

Slightly higher outlet pressure, approximately 4.5, is expected when redundant measurement equipment is removed. In addition, the superheat from the second compressor is used to heat the drying agent slightly above the saturation temperature of the steam.

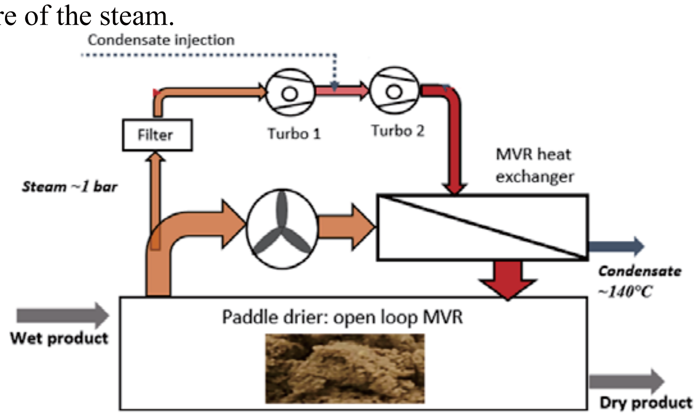

Figure 6: Illustration of the soon to be tested industrial MVR dryer with a two stage turbo compressor setup

http://dx.doi.org/10.18462/iir.gl.2020.1019

4. CONCLUSIONS

A two stage turbo compressor configuration for an open loop steam dryer has been experimentally verified in close to industrial conditions. The compressor prototypes are supplied by ROTREX™ and are based on affordable, mass produceed air compressors for the automotive industry. The experimental results presented in this paper concludes that the two stage configuration is able to lift the saturation temperature from 100°C to 146°C, 1 bar to 4.2 bar. Even higher temperature lift is enabled when redundant measurement equipment is removed. In addition, the superheat from the second compressor is used to heat the drying agent slightly above the condensation temperature of the steam. The COP of the system was calculated to be 4.54, resulting in 80% electricity reduction compared to a 90% efficient electrically driven steam generator. The compressors are planned to be demonstrated in an industrial dryer during 2020, which will lead to further experimental verification.

ACKNOWLEDGEMENTS

This work is a part of the DryFiciency project (www.dry-f.eu). DryFiciency receives funding from the European Commission under the Horizon 2020 programme - grant number 723576.

NOMENCLATURE

p	pressure (kPa)	h	enthalpy ($kJ \times kg^{-1}$)
T	temperature (K)	$\dot{m}$	mass flow ($kg \times s^{-1}$)
ρ	density ($kg \times m^{-3}$)	Q_c	condenser heat (kW)
W_{el}	Compressor Work (kW)		

REFERENCES

Arpagaus, C, et. al, 2018, High Temperature Heat Pumps: Market Overview, State of the Art, Research Status, Refrigerants, and Application Potentials. Int. Refrigeration and Air Conditioning Conference. Paper 1876.

Bantle, M., Schlemminger, C., Gabrielli, C., Arhens, M., 2019, Turbo-compressors for R-718: Experimental evaluation of a two-stage steam compression cycle, Proceedings of the 25th IIR International Congress of Refrigeration. Montréal, Canada, p. 4567 – 4574.

Di Wu, Jiatong Jiang, Bin Hu, R.Z. Wang, 2020, Experimental investigation on the performance of a very high temperature heat pump with water refrigerant, Energy, Volume 190

Elmegaard, B., Zühlsdorf, B., Reinholdt, L., & Bantle, M., 2017, Book of presentations of the International Workshop on High Temperature Heat Pumps. Kgs. Lyngby: Technical University of Denmark

Gutierrez-Lopez, Gustavo F., 2003, Food Science and Food Biotechnology, CRC Press, pp 274,

Hafaifa, A., Rachid, B., Mouloud, G., 2014. Modelling of surge phenomena in a centrifugal compressor: experimental analysis for control, Systems Science & Control Engineering, p. 632-641.

Larminat, P. et al, 2014. A high temperature heat pump using water vapor as working fluid. 11th IIR Gustav Lorentzen Conference on Natural Refrigerants. Hangzhou, China.

Madsbøll, H., 2015, Development of Water Vapor Compressors and future market implementation, IEA Heat Pump Workshop @DTI, https://www.osti.gov/etdeweb/servlets/purl/22059284

Šarevski, M, Šarevski V., 2017, Thermal characteristics of high-temperature R718 heat pumps with turbo compressor thermal vapor recompression. Applied Thermal Engineering, p 355-365. doi:101016/japplthermaleng201702035

Weel. M, Mikkelsen J., Johansson M, 2012, Industrielle varmepumpe for høje temperaturer (in danish), Report in research project

http://dx.doi.org/10.18462/iir.gl.2020.1019